© 2022. Published by The Company of Biologists Ltd | Journal of Experimental Biology (2022) 225, jeb243599. doi:10.1242/jeb.243599

RESEARCH ARTICLE

The relationship between head shape, head musculature and bite force in caecilians (Amphibia: Gymnophiona)

Aurélien Lowie[1,‡], Barbara De Kegel[1], Mark Wilkinson[2], John Measey[3], James C. O'Reilly[4], Nathan J. Kley[5], Philippe Gaucher[6], Jonathan Brecko[7], Thomas Kleinteich[8], Dominique Adriaens[1,*] and Anthony Herrel[1,9,*]

ABSTRACT

Caecilians are enigmatic limbless amphibians that, with a few exceptions, all have an at least partly burrowing lifestyle. Although it has been suggested that caecilian evolution resulted in sturdy and compact skulls as an adaptation to their head-first burrowing habits, no relationship between skull shape and burrowing performance has been demonstrated to date. However, the unique dual jaw-closing mechanism and the osteological variability of their temporal region suggest a potential relationship between skull shape and feeding mechanics. Here, we explored the relationships between skull shape, head musculature and *in vivo* bite forces. Although there is a correlation between bite force and external head shape, no relationship between bite force and skull shape could be detected. Whereas our data suggest that muscles are the principal drivers of variation in bite force, the shape of the skull is constrained by factors other than demands for bite force generation. However, a strong covariation between the cranium and mandible exists. Moreover, both cranium and mandible shape covary with jaw muscle architecture. Caecilians show a gradient between species with a long retroarticular process associated with a large and pennate-fibered m. interhyoideus posterior and species with a short process but long and parallel-fibered jaw adductors. Our results demonstrate the complexity of the relationship between form and function of this jaw system. Further studies that focus on factors such as gape distance or jaw velocity will be needed in order to fully understand the evolution of feeding mechanics in caecilians.

KEY WORDS: Cranial morphology, Feeding mechanics, Muscle architecture, Geometric morphometrics

INTRODUCTION

Caecilians (Gymnophiona) are a small (>210 currently recognized species) monophyletic group of elongate, totally limbless and annulated amphibians (Pough et al., 1998; Taylor, 1968). Because most caecilians are fossorial, inconspicuous and rarely encountered components of tropical ecosystems, many aspects of their biology are poorly known (O'Reilly, 2000; Summers and O'Reilly, 1997; Wilkinson, 2012). Of the 10 currently recognized families (Wilkinson et al., 2011; Kamei et al., 2012), only Typhlonectidae includes fully aquatic species, species of other families being primarily terrestrial as adults. With a few exceptions, caecilians are head-first burrowers (Taylor, 1968), which imposes specific constraints on the cranial system of limbless vertebrates (O'Reilly, 2000; Wake, 1993). Their typically compact, robust crania, with several composite (fused) bones and tight sutures, have been interpreted as adaptations for head-first burrowing (e.g. Wake, 1993; Wake and Hanken, 1982; Wilkinson, 2012). Although some features of the skull, such as the bony covering of the eye, the position of the mouth and the fenestration of the skull, are probably adaptations to head-first digging, no relationship between skull shape and burrowing force has been demonstrated to date (Ducey et al., 1993; Herrel and Measey, 2010; Kleinteich et al., 2012; Lowie et al., 2021).

Given that the cranium also plays roles in multiple other functions, such as feeding, lung ventilation and housing the brain and major sensory organs (Wake, 1993), it is thus expected to be shaped by many, possibly competing, functional demands. Whereas frogs (Anura) and salamanders (Caudata) show a variety of feeding mechanisms, all terrestrial caecilians studied use jaw prehension, while aquatic caecilians also use suction feeding (O'Reilly, 2000). Although observations of *in vivo* feeding behavior are scarce, caecilians are thought to be generalist and opportunistic predators, feeding mostly on earthworms and subterranean arthropods (Taylor, 1968; Wake, 1980; Verdade et al., 2000; Delêtre and Measey, 2004; Gaborieau and Measey, 2004; Measey et al., 2004; Kupfer et al., 2005; Herrel and Measey, 2012; Kouete and Blackburn, 2020; but see Moll and Smith, 1967; Presswell et al., 2002; Govindappa and Parwar, 2016, for occurrences of lizards, snakes and other caecilians in the diet of caecilians). The high modularity of the temporal region (Bardua et al., 2019b) and streptostyly observed in caecilian skulls (Kleinteich et al., 2008b; Summers and Wake, 2005; Wake and Hanken, 1982) does, however, suggest a potential relationship between variation in skull shape and feeding mechanisms (Summers and Wake, 2005).

Because of the totally (stegokrotaphic) or partially (zygokrotaphic) closed temporal region and the severe constraints that head-first burrowing puts on the maximal head diameter (Bemis et al., 1983; Gans, 1974; O'Reilly, 2000), the laterally placed external jaw adductor muscles are constrained in size by bones and strongly reduced compared with those of other amphibians (Bemis et al., 1983; Nussbaum, 1977, 1983; O'Reilly, 2000). However, caecilians possess a unique jaw-closing system involving the large and well-developed m. interhyoideus posterior

[1]Ghent University, Department of Biology, Evolutionary Morphology of Vertebrates, K.L. Ledeganckstraat 35, 9000 Gent, Belgium. [2]Department of Life Sciences, Natural History Museum, London SW7 5BD, UK. [3]Centre for Invasion Biology, Department of Botany & Zoology, Stellenbosch University, Private Bag X1, 7602 Matieland, Stellenbosch, South Africa. [4]Department of Biomedical Sciences, Ohio University, Cleveland Campus, SPS-334C, Cleveland, OH 45701, USA. [5]Department of Anatomical Sciences, Health Sciences Center, T8-082, Stony Brook University, Stony Brook, NY 11794-8081, USA. [6]USR 3456, CNRS, Centre de recherche de Montabo IRD, CNRS-Guyane, 97334 Cayenne, France. [7]Royal Museum for Central Africa, Biological Collections and Data Management, 3080 Tervuren, Belgium. [8]TPW Prufzentrum GmbH, 41460 Neuss, Germany. [9]UMR 7179 C.N.R.S./M.N.H.N., Département d'Ecologie et de Gestion de la Biodiversité, 57 rue Cuvier, Case postale 55, 75231 Paris Cedex 5, France.
*These authors contributed equally to this work.

‡Author for correspondence (aurelien.lowie@UGent.be)

A.L., 0000-0003-0065-7152; M.W., 0000-0002-9459-8976; J.M., 0000-0001-9939-7615; D.A., 0000-0003-3610-2773; A.H., 0000-0003-0991-4434

Received 27 September 2021; Accepted 6 December 2021

Journal of Experimental Biology (2022) 225, jeb243599. doi:10.1242/jeb.243599

(Bemis et al., 1983; Nussbaum, 1977, 1983). This pennate-fibered muscle is positioned in such a way that its physiological cross-section can be increased without a corresponding increase in head diameter (Nussbaum, 1977, 1983; Bemis et al., 1983; O'Reilly, 2000; Herrel et al., 2019). These morphological features suggest that caecilians can generate considerable bite forces (Herrel et al., 2019; Kleinteich et al., 2008a,b; Measey and Herrel, 2006; Summers and Wake, 2005). Preliminary bite force data presented by Herrel et al. (2019) suggest that the jaw-closing system may be different across caecilians, yet little is known about variation in the jaw muscles and its impact on bite force.

Using 3D geometric morphometrics and quantitative data on cranial muscles [mass, fiber length and physiological cross-sectional area (PCSA)], we investigated the relationships between skull shape, jaw musculature and bite force of 28 species of caecilian amphibians. As shape variation in the cranium and the mandible has already been described by Lowie et al. (2021), only shape covariation was assessed in this study. Whereas the cranium plays a vital role in many activities, the lower jaw is mainly involved in biting and respiration (Carrier and Wake, 1995; Wake, 1993). Consequently, we predicted a stronger covariation between the PCSA of the jaw muscles and mandibular shape than between the PCSA of the jaw muscles and cranial shape. However, we expected the shape of the cranium to covary more with the muscle volume because it reflects architectural constraints imposed by the partial or complete closure of the temporal area. We also investigated the relationships between *in vivo* bite forces and both skull shape and jaw muscle architecture in caecilians. We predicted that species with a more pronounced and more curved retroarticular process, and thus a greater input lever for the jaw-closing m. interhyoideus posterior, will produce more force (Summers and Wake, 2005). We further predicted that variation in the m. interhyoideus posterior will be the principal driver of variation in bite force as it is the largest jaw-closing muscle. Finally, we predicted that aquatic species using suction feeding will show lower bite forces, yet may possess longer muscle fibers as suction feeding probably puts strong demands on jaw-closing velocity.

MATERIALS AND METHODS

Specimens

We quantified the shape of the cranium and mandible of 81 individuals from 28 species belonging to nine out of the 10 currently recognized families (Table 1), thus capturing a broad diversity in cranial osteology, phylogeny and ecology. Our sample was restricted to adults and included both males and females. Although some sexual dimorphism is present in caecilians (e.g. Kupfer, 2009; Maerker et al., 2016), interspecific variation largely exceeds the sex-specific variation (Sherratt et al., 2014). Specimens were obtained primarily from our personal collections and completed with specimens from museum collections (Tables S1 and S2).

Bite force

In vivo bite forces were measured in the field for 139 specimens belonging to 11 species (Table 2). Wild-caught specimens were maintained for a maximum of 24 h in large containers filled with substrate collected in the field at sites where the animals were found. Some species (*Dermophis mexicanus*, *Ichthyophis* sp., *Schistometopum thomense*, *Geotrypetes seraphini*, *Herpele squalostoma* and *Boulengerula taitanus*) were maintained under laboratory conditions for longer time periods (months or years), in large tubs with soil and fed with earthworms and crickets. After

Table 1. Details of specimens used in this study, with family, species and number of individuals for each dataset

		No. of individuals				
Family	Species	Cranium	Mandible	Bite force	Morphometrics	Dissections
Caeciliidae	*Caecilia museugoeldi**	1	1	2	4	0
	*Caecilia tentaculata**	2	2	1	2	0
Dermophiidae	*Dermophis mexicanus**	4	4	19	22	2
	*Geotrypetes seraphini**	5	5	12	19	7
	Schistometopum gregorii	1	1	0	0	0
	*Schistometopum thomense**	4	4	12	16	3
Herpelidae	*Boulengerula boulengeri*	1	1	0	0	0
	*Boulengerula fischeri**	5	5	4	31	4
	*Boulengerula taitanus**	5	5	44	62	10
	*Herpele squalostoma**	5	5	8	14	5
Ichthyophiidae	*Ichthyophis bombayensis*	1	1	0	0	0
	*Ichthyophis kohtaoensis**	4	4	7	9	2
	Uraeotyphlus oxyurus	1	1	0	0	0
Indotyphlidae	*Gegeneophis ramaswamii*	4	4	0	0	0
	Grandisonia alternans	4	4	0	0	0
	Hypogeophis rostratus	4	4	0	4	0
	Sylvacaecilia grandisonae	1	1	0	0	0
Rhinatrematidae	*Epicrionops bicolor*	1	1	0	0	0
	*Rhinatrema bivittatum**	5	5	17	21	4
Scolecomorphidae	*Scolecomorphus kirkii*	1	1	0	0	0
	Scolecomorphus uluguruensis	6	4	0	0	0
Siphonopidae	*Microcaecilia unicolor*	2	2	0	0	0
	Mimosiphonops vermiculatus	1	1	0	0	0
	Siphonops annulatus	3	3	0	1	0
Typhlonectidae	*Atretochoana eiselti*	2	2	0	0	0
	Potomotyphlus kaupii	2	2	0	0	0
	*Typhlonectes compressicauda**	5	5	13	18	2
	Typhlonectes natans	1	1	0	1	0

*Species for which *in vivo* data were available and included in the subsampled dataset.

Table 2. Morphometrics and bite force of the specimens used in the study

Species	Mass (g)	SVL (mm)	HL (mm)	HW (mm)	HH (mm)	LJL (mm)	BW (mm)	Max. bite force (N)
Boulengerula fischeri	2.62±0.93	259.79±61.25	4.32±0.67	2.61±0.33	1.9±0.26	3.04±0.65	3.02±0.5	0.12±0.02
Boulengerula taitanus	5.64±2.17	270.38±42.35	6.68±0.85	3.91±0.55	2.76±0.41	5.23±1.3	5.04±0.95	1.88±1.32
Caecilia museugoeldi	21.7*	410.5±160.37	11.51±1.98	7.78±1.12	5.39±0.81	8.95±1.44	10.24±0.11	3.66±0.6
Caecilia tentaculata	149*	645.5±106.77	20.52±0.64	14.42±0.52	10.01±2.02	16.52±1.14	19.17	7.11
Dermophis mexicanus	105.44±53.6	416.23±61.79	16.43±1.91	13.91±2.08	8.83±1.02	16.68±2.9	18.85±4.22	11.36±2.79
Geotrypetes seraphini	11.13±5.5	213.37±34.65	7.85±1.09	4.98±0.66	3.25±0.35	6.51±0.81	7.43±1.24	1.57±0.85
Herpele squalostoma	10.27±3.99	249.21±36.51	8.04±0.96	5.27±0.79	3.58±0.78	6.89±0.91	6.6±1.13	2.03±0.99
Ichthyophis kohtaoensis	19.17±8.51	318.89±51.04	10.5±0.89	7.48±0.57	4.79±0.17	10.78±1.1	7.15±0.5	4.64±1
Rhinatrema bivittatum	9.25±3.3	203±31.23	9.02±0.7	5.62±0.49	3.55±0.37	8.8±0.7	7.37±1.31	1.38±0.52
Schistometopum thomense	5.87±2.94	207.75±25.9	8.3±0.8	5.11±0.56	3.57±0.3	7.79±0.99	6.47±0.96	1.09±0.32
Typhlonectes compressicauda	33.25±20.78	301.22±62.35	13.34±2.15	8.68±1.23	5.25±0.68	10.58±1.64	12.28±3.06	1.22±0.51

Data are means±s.d. SVL, snout–vent length; HL, head length; HW, head width; HH, head height; LJL, lower jaw length; BW, body width. For the number of individuals used, see Table 1. *Mass was available for only one individual for these species.

measurements, field-caught animals were released at the exact locations where they were found. Bite forces were measured using an isometric Kistler force transducer (type 9203, ±0.01 N; Kistler, Zurich, Switzerland) mounted on a purpose-built holder and connected to a Kistler charge amplifier (type 5995A, Kistler; see Herrel et al., 1999, 2001, for a detailed description of the set-up; Fig. 1). The free end of the holder was placed between the jaws of the animal, which immediately resulted in a fierce and prolonged biting. The place of application of the force and gape angle (roughly 20 deg), were standardized. Each animal was tested at least 5 times, with an interval of at least 30 min between trials. The maximal value recorded was considered as the maximal *in vivo* bite force of the animal, which was then used for subsequent analyses.

Dissection and muscle properties

Five head muscles that contribute to the unique dual jaw-closing system in caecilians (Nussbaum, 1983) were examined in this study: the m. adductor mandibulae internus (MAMI), longus (MAML) and articularis (MAMA), the m. interhyoideus posterior (MIHP) and the m. pterygoideus (MPt). Additionally, the well-developed m. depressor mandibulae (MDM) was included in the analyses as it probably plays a role in shaping the cranium and the mandible (Fig. 2). Muscle nomenclature is based on homologies with jaw musculature in other amphibians and in caecilian larvae (Haas, 2001; Kleinteich and Haas, 2007; Theska et al., 2018). Prior to dissection, specimens used for morphological analyses that were stored in a 70% aqueous ethanol solution were rehydrated in water for 15–20 min. Muscles were removed unilaterally from each specimen under a dissecting microscope (Wild M3Z, Wild Inc., Muttenz, Switzerland) and weighed using a digital microbalance (Sartorius CP225D ±10 µg). Muscle fiber lengths were obtained by submerging the muscles in a 30% nitric acid solution (30% HNO_3) for 24 h to dissolve all connective tissue. Muscle fibers were then put in a 50% glycerol solution and at least 10 fibers for every muscle were drawn using a dissecting microscope with *camera lucida*. Drawings were then scanned and fiber lengths were quantified using ImageJ 1.52a (Wayne Rasband, National Institutes of Health, Bethesda, MD, USA). Next, we calculated the average length of the fibers for each muscle. Finally, the PCSA of each muscle was calculated as follows:

$$\mathrm{PCSA} = \frac{\text{muscle mass} \times \cos\alpha(\text{pennation angle})}{\text{muscular density} \times \text{fiber length}}, \quad (1)$$

where muscle mass is in g, pennation angle is in rad, muscular density is in g cm^{-3} and fiber length is in cm. A fixed muscular density of 1.06 g cm^{-3} (Mendez and Keys, 1960) was assumed. Pennation angles were obtained from the contrast enhanced micro-computed tomography (µCT) scans (see 'µCT imaging', below). A summary of the muscle measurements is provided in Table S3.

µCT imaging

For this study, CT scans of different species were used (Table S1). About half of these scans were performed at the Centre for X-Ray Tomography at Ghent University, Belgium (UGCT, www.ugct.ugent.be) using the HECTOR µCT scanner (Masschaele et al., 2013). The scanner settings were sample dependent. The tube voltage varied between 100 and 120 kV and the number of X-ray projections taken over 360 deg was typically about 2000 per scan. Additional µCT scans were obtained from the online repository Morphosource (morphosource.org), the Zoological Museum Hamburg (see Kleinteich et al., 2008a, for scanner settings), the Royal Museum of Central Africa (75 kV, 1440 projections), and the personal collection of M.W. (100 kV, 3142 projections; see Table S1). The isotropic voxel size of all scans is listed in Table S1. All the µCT scans were processed using both automatic thresholding and manual segmentation to reconstruct the cranium and mandible in 3D using Amira 2019.3 (Visage Imaging, San Diego, CA, USA). Using Geomagic Wrap (3D systems), surfaces were prepared by removing highly creased edges and spikes that may interfere with the placement of landmarks. Next, they were decimated to a maximum of approximately 700,000 faces to reduce computational demands without compromising details. For the mandible, only the left hemimandible was used. The 'mirror' function in Geomagic was used for the specimens where the left hemimandible was damaged.

We also used 11 specimens from different species for soft tissue visualization. Specimens were stained using either a 2.5% phosphomolybdic acid (PMA) solution or a 6% Lugol's iodine (I_2KI) solution (Descamps et al., 2014; Gignac et al., 2016; Table S2). The staining time varied from 14 to 21 days depending on the size of the specimen. All specimens were then scanned with the HECTOR µCT scanner (100 kV, 2400 projections; Table S2). After a fully manual segmentation in Amira 2019.3, muscles volume was computed using the 'Material Statistics' module. The contrast threshold was then manually lowered for each muscle in order to highlight muscles fibers. The fiber length of all the muscles

Journal of Experimental Biology (2022) 225, jeb243599. doi:10.1242/jeb.243599

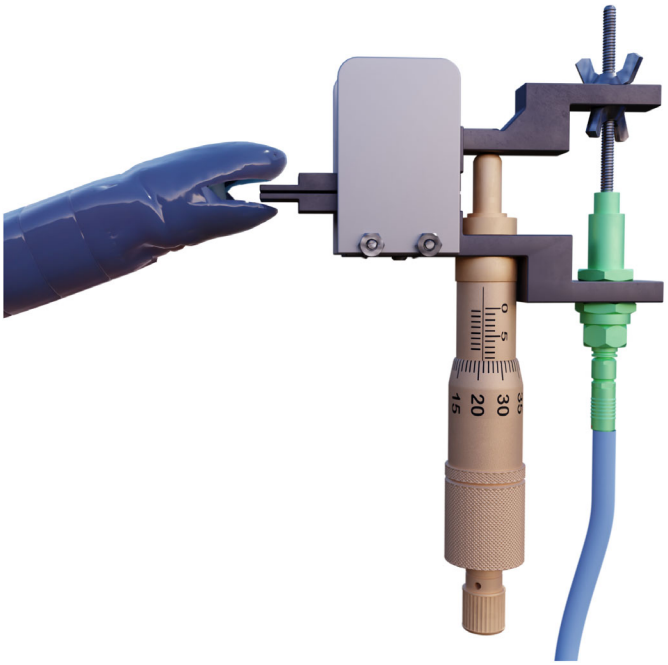

Fig. 1. Experimental set-up. Schematic illustration of the set-up used to measure biting forces. The free ends of the metal holder (dark gray) were placed between the jaws of the animal to induce biting. Biting causes the upper plate to pivot around the micrometer head acting as a fulcrum (light brown). The force was then transmitted to the force transducer (green).

and pennation angle of the MIHP and the MDM were measured using the standard measure tool in Amira. Average fiber length and pennation angle were calculated based on at least 10 fibers per muscle. The PCSA was then calculated by dividing muscle volume by muscle length and multiplied by the cosine of the pennation angle when applicable.

3D geometric morphometrics

In addition to anatomical landmarks, we also used 3D sliding semi-landmarks on curves (Bardua et al., 2019a; Bookstein, 1991; Buser et al., 2018; Fabre et al., 2018, 2015; Gunz et al., 2005). Both kinds of landmark were placed manually onto the crania and mandibles, by the same person (A.L.) using Stratovan Checkpoint (Stratovan corporation, v. 2020.10.13.0859). Nineteen homologous landmarks and two curves were placed on the left hemimandible and 88 homologous landmarks and four curves on the cranium (see Lowie et al., 2021, for a detailed and illustrated description of the landmarking process). Curves were resampled (see Botton-Divet et al., 2016, for a detailed description of the method) and all the sliding semi-landmarks were slid while minimizing the bending energy using the 'slider3d' function from the Morpho R package v. 2.8. Finally, a generalized Procrustes analysis (GPA) was performed using the 'gpagen' function from the Geomorph R package v. 3.3.1.

Morphometrics

External measurements were collected on all specimens used in the biting trials to characterize their external morphology. Head length from the tip of the snout to the back of the parietal bone, head width at the widest point of the head just anterior to the jaw articulation, head height at the tallest point of the head, lower jaw length measured from the tip of the jaw to the back of the retroarticular process, and body width at mid-body were measured using a digital caliper (Mitutoyo, precision ±0.01 mm). Emaciated specimens were not included. The snout–vent length was measured by stretching the animals along a ruler (±1 mm). Individuals were also weighed using an electronic balance or a spring scale (Ohaus, precision ±0.01 g) (Table 2).

Phylogeny

Because species are not independent data points, their phylogeny was taken into account in our comparative analyses (Felsenstein, 1985). The phylogenetic tree of Jetz and Pyron (2018) was pruned to only include the species used in our study. Using 10,000 trees from VertLife.org, the maximum credibility tree was computed using the 'maxCladeCred' function in the Phangorn package in R (http://www.R-project.org/).

Statistical analyses

All the statistical analyses were performed in R v. 4.0.3 (http://www.R-project.org/). The significance threshold was set at α=0.05. External measurements, muscle data and bite forces were transformed logarithmically ($\log_{10}$) to fulfill assumptions of normality and homoscedasticity.

To assess the impact of size on shape, we performed a Procrustes regression on the GPA coordinates using the 'procD.lm' function from the Geomorph package. The $\log_{10}$ centroid size was used as a proxy for size. Residuals for both cranium and mandible were then computed and further referred to as allometry-free shapes, in order to examine shape variation not attributable to allometry.

To visualize the evolutionary patterns of shape variation in the cranium and mandible, we performed a principal component analysis (PCA) on the mean of the allometry-corrected shapes for each species using the 'gm.prcomp' function from the Geomorph package. Then, we projected the phylogeny onto the morphospace. The results of shape allometry and the principal axes of shape variation of the cranium and the mandible are described in Lowie et al. (2021).

To estimate the degree of similarity due to shared ancestry, a multivariate *K*-statistic (Adams, 2014) was calculated on the mean Procrustes coordinates of the cranium, the mandible, the muscles (length, volume and PCSA) and the external measurements using the 'physignal' function in the Geomorph package. A univariate *K*-statistic was calculated on the forces using the 'phylosig' function in the Phytools package. The phylogenetic signal was calculated under the assumption of Brownian motion (Blomberg et al., 2003). The higher the *K*-value, the stronger the phylogenetic signal. Values of $K>1.0$ describe data with a greater phylogenetic signal than expected from Brownian motion alone.

A phylogenetic two-block partial least-squares (2B-PLS) analysis, with the allometry-free cranial shapes in a first block and the allometry-free mandibular shapes in a second block, was performed in order to assess the covariation between the cranium and mandible in caecilians.

Phylogenetic generalized least-squares (PGLS) regressions were performed in order to assess the relationships between external measurements and bite force using the 'procD.pgls' function from the Geomorph package. As head width was highly correlated with bite force (see Results; Table 3) and is biomechanically relevant for bite force (e.g. Le Guilloux et al., 2021; Vanhooydonck et al., 2011), residuals of the skull shape (cranium and mandible), bite force and muscles (length, volume and PCSA) were computed using

Journal of Experimental Biology (2022) 225, jeb243599. doi:10.1242/jeb.243599

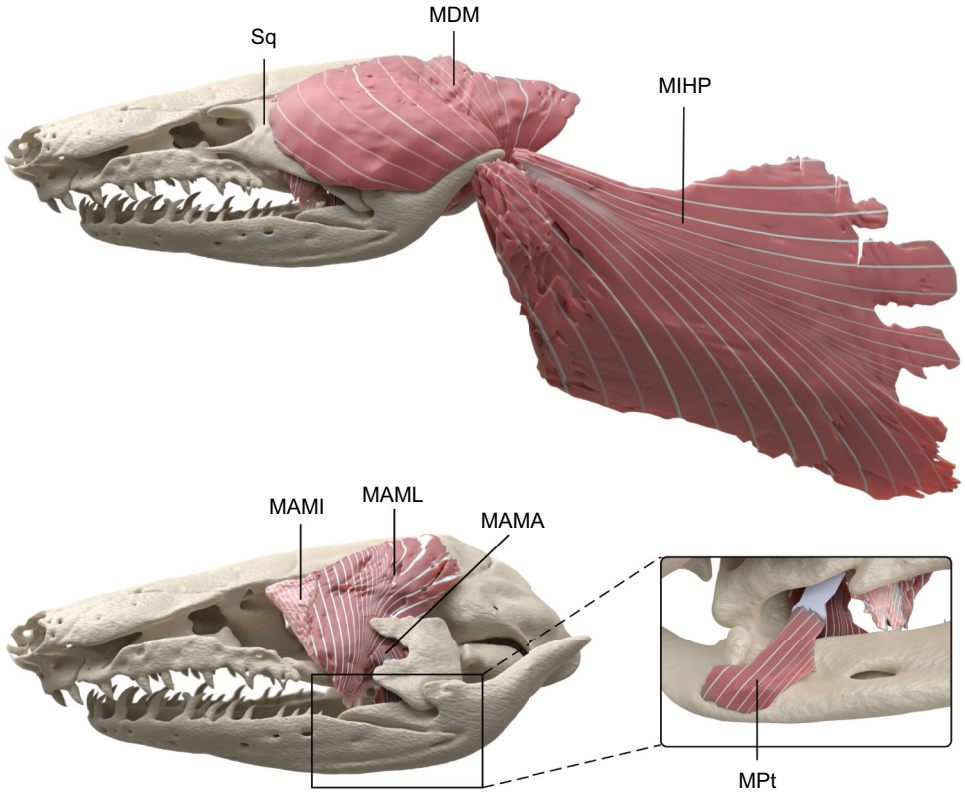

Fig. 2. Skull and associated head musculature in *Geotrypetes seraphini*. Top: left lateral view of the skull and associated musculature: the m. depressor mandibulae (MDP), the m. interhyoideus posterior (MIHP) and the squamosal bone (Sq). Bottom: the MDP, MIHP and Sq were removed to visualize the underlying musculature: m. adductor mandibulae internus (MAMI), m. adductor mandibulae longus (MAML) and m. adductor mandibulae articularis (MAMA). The inset is a close-up view of the medial side of the mandible, showing the m. pterygoideus (MPt).

Table 3. Results of the phylogenetic linear regressions between external measurements and maximum bite force

	R^2	P
Mass	0.62	**0.004**
Snout–vent length	0.43	**0.035**
Head length	0.67	**0.004**
Head width	0.71	**0.002**
Head height	0.7	**0.003**
Lower jaw length	0.73	**0.002**
Body width	0.68	**0.003**

Bold indicates significance.

PGLS regressions with head width as co-factor and further referred to as residuals.

Next, the relationships between the residuals of cranial and mandibular shape and the residuals of bite force were assessed using PGLS regressions.

To quantify the covariation between bite force and the jaw-closing muscles (length, volume and PCSA of the MAML, MAMI, MAMA, IHP and MPt), phylogenetic 2B-PLS analyses were performed using the 'phylo.integration' function from the Geomorph package, with the residuals of bite force as one block and the residuals of the muscle parameters (length, volume or PCSA) as the second block.

Finally, the covariation between skull shape (cranium and mandible) and the head muscles (length, volume and PCSA of the MAML, MAMI, MAMA, IHP, MPt and MDM) was quantified using 2B-PLS, with the residuals of the shape (cranium or mandible) in one block and the residuals of the muscles (length, volume or PCSA) in the second block.

Ethics statement

None of the measurements described in this paper (force measurements or external morphometrics) are considered procedures requiring ethics approval under European law. Furthermore, no permits are needed to maintain caecilians in captivity in Europe. All wild-caught animals were maintained for one night and one day, checked for signs of stress and released at their exact site of capture (marked by GPS) the next night. Captive animals were maintained individually in large tubs of soil in a climate-controlled room (24°C) and fed with earthworms and crickets twice weekly. Animals were checked for signs of stress and injury after bite force measurements and monitored for signs of weight loss during the following weeks. None of the animals were harmed, or showed any signs of stress or weight loss after measurements, and all measurements were approved by local animal care and use committees.

RESULTS

Phylogenetic signal

The multivariate K-statistic calculated for the cranium (K_{mult}=0.83, P=0.001) and mandible (K_{mult}=0.88, P=0.001) was significant, but the signal was moderate (K<1). However, no significant phylogenetic signal was detected for the muscles (length: K_{mult}=0.63, P=0.55; volume: K_{mult}=0.65, P=0.54; PCSA: K_{mult}=0.69, P=0.44), the external measurements (K_{mult}=0.62, P=0.57), or bite force (K=0.65, P=0.53).

Covariation between skull and mandible

The phylogenetic 2B-PLS analysis performed on the allometry-free shapes showed a strong and significant covariation between the cranium and the mandible (P=0.001, r-PLS=0.91; Fig. 3). The positive extremes of the scatterplot, mostly driven by the aquatic

Journal of Experimental Biology (2022) 225, jeb243599. doi:10.1242/jeb.243599

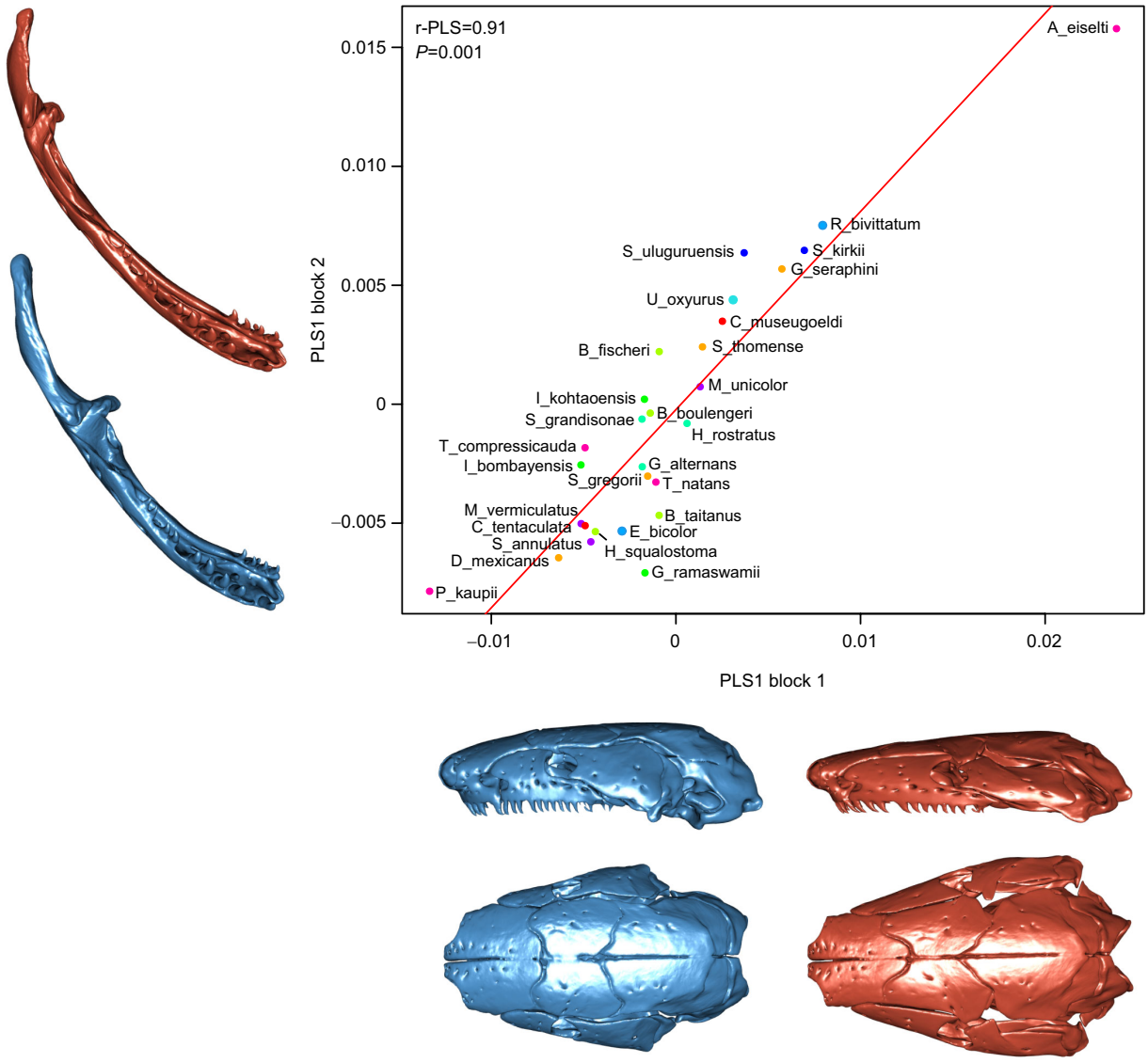

Fig. 3. Results of the phylogenetic two-block partial least-squares (2B-PLS) analysis of cranial shape and mandibular shapes (*n*=81). Scatter plot of the first PLS axis describing the covariation between mandible and cranium shape. Circles represent species means (*n*=28) and are colored by clade. The warped surfaces represent the shape covariation associated with the extreme of the principal components (blue, minimum extreme; red, positive extreme). For full species names, see Table 1.

Atretochoana eiselti, represent species with long and posteriorly projected quadrates that covary with slender mandibles with a proportionately small and dorso-medially curved retroarticular process and relatively posteriorly positioned articulation. The negative part of the plot represents species for which small quadrates covary with mandibles having a longer retroarticular process associated with the shift of the articulation toward the front of the mandible (Fig. 3).

Variation in bite force

Absolute maximal bite force across the 11 species included in the study ranged from 0.12±0.02 N for *Boulengerula fischeri*, the smallest species in our dataset, to 11.36±2.79 N for *Dermophis mexicanus*, one of the biggest species in our dataset (see Table 2). The PGLS regressions showed a significant relationship between maximum bite force and the external head measurements (Table 3). For a given head width, *Boulengerula taitanus* and *Ichthyophis kohtaoensis* had the highest bite forces while the aquatic *Typhlonectes compressicauda* had the lowest bite force, closely followed by *B. fischeri* (Fig. 4).

Relationship between muscles and force

Results of the phylogenetic 2B-PLS analysis showed no covariation between residual bite force and residual muscle fiber length (P=0.07, r-PLS=0.76). However, a significant covariation was observed for the residuals of muscle volume (P=0.05, r-PLS=0.74). Species present on the negative part of the plot have bigger MAMI, MIHP, MAML and MAMA and slightly smaller MPt covarying with higher bite forces (Fig. 5A). Muscle PCSA showed the strongest covariation with bite force (P=0.02, r-PLS=0.82). For both volume and PCSA, MAMI and MIHP were the principal drivers of the covariations. Species present on the negative part of the plot have larger PCSA values (except for MPt which negatively covaries with bite force) and higher bite forces (Fig. 5B).

Journal of Experimental Biology (2022) 225, jeb243599. doi:10.1242/jeb.243599

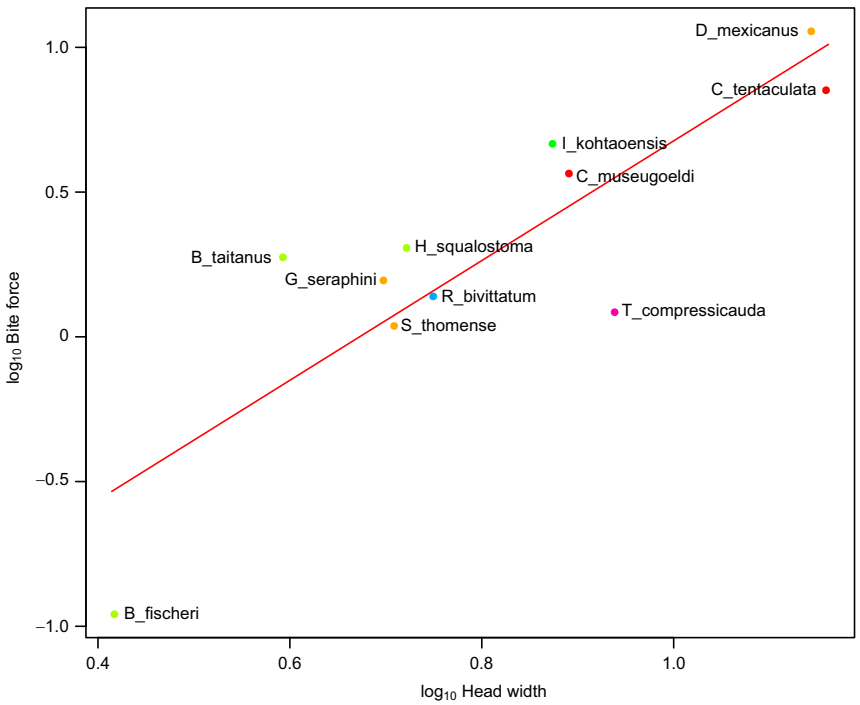

Fig. 4. Scatterplot showing the relationship between head width and maximal bite force in caecilians (*n*=139). Circles represent species means (*n*=11) and are colored by clade. For full species names, see Table 1.

Relationship between skull shape and force

The results of the PGLS analyses showed no correlation between residual skull shape and residual bite force (cranium: P=0.9, R^2=0.06; mandible: P=0.8, R^2=0.07).

Relationship between skull shape and muscles

The results of the phylogenetic 2B-PLS analysis showed a significant covariation between the residual cranial shape and the residual muscle fiber length (P=0.017, r-PLS=0.94). The main muscles contributing to the covariation with cranial shape are the MAMI, MPt and MDM. Toward the positive extreme, the shape covariation observed corresponds mainly to a shortening of the os basale and the maxillary bones associated with shorter fibers in the MAMI and MDM but longer MPt fibers (Fig. 6). A slight widening of the braincase, and thus closing of the temporal region, was also observed for species occupying the positive part of the plot (Fig. 6). Additionally, species on the positive extreme have broader interdental plates of the maxillary. Interestingly, no significant covariation was observed between cranial shape and muscle volume (P=0.07, r-PLS=0.90) or muscle PCSA (P=0.27, r-PLS=0.86).

For the mandible, a significant covariation was found between residual mandibular shape and residual muscle volume (P=0.04, r-PLS= 0.90). The main muscles contributing to the covariation with mandibular shape were the MAMI, MAMA and MPt. Toward the positive extreme, the shape covariation observed corresponds to slender and straighter mandibles with short retroarticular processes associated with a large MAMI, MAMA and MPt, but a smaller MIHP (Fig. 7). The negative part shows more medially curved and bulky mandibles with longer retroarticular processes associated with larger MIHPs. No significant co-variation was observed between residual mandible shape and the length (P=0.1, r-PLS=0.88) or PCSA (P=0.19, r-PLS=0.85) of the muscles.

DISCUSSION

Covariation between cranium and mandible

Our results show a strong covariation between cranial and mandibular allometry-free shapes. One extreme is driven by the unusual aquatic caecilian *Atretochoana eiselti* (see Wilkinson and Nussbaum, 1997). The quadrate bones in *A. eiselti* are caudally and ventrally elongated, unlike in other caecilians (Wilkinson and Nussbaum, 1997). This quadrate elongation covaries with a posterior displacement of the jaw articulation, leading to a short retroarticular process and a very long pseudodentary. As mentioned by Wilkinson and Nussbaum (1997), this shift of the articulation presumably allows for an increased gape and the capture of relatively large prey. A shorter retroarticular process probably also corresponds to a shift in the use of the adductors as the primary mechanism of jaw closing. This is not unsurprising as aquatic species are not feeding in confined tunnels and thus are freed from the need to reduce the width of their head. This is supported by the relatively low bite forces observed in the aquatic suction feeder *Typhlonectes compressicauda*. Species with a longer retroarticular process may switch toward the use of the MIHP as the primary mode of jaw closing as the moment arm provided by the retroarticular process becomes greater with an increase in the length of the retroarticular process.

Relationship between shape and bite force

Several studies have highlighted the variability of the quadrate–squamosal complex and have suggested a potential relationship between skull shape and feeding mechanisms (Bardua et al., 2019b; Kleinteich et al., 2008b; Lowie et al., 2021; Summers and Wake, 2005; Wake and Hanken, 1982). Although the main axes of shape variation observed in caecilian skulls are described by changes occurring in the tooth-bearing bones, the temporal region and the quadrate–squamosal complex (Bardua et al., 2019b; Lowie et al., 2021; Sherratt et al., 2014), no relationship between *in vivo* bite force and cranium shape was found. This suggests that the shape of the skull in caecilians is constrained by factors other than demands for bite force generation.

As observed in previous studies (e.g. Wake, 2003) and confirmed by Lowie et al. (2021), the main axis of shape variation in the mandible is the length of the retroarticular process and the angle it forms with the pseudodentary. Modeling studies focusing on the

Journal of Experimental Biology (2022) 225, jeb243599. doi:10.1242/jeb.243599

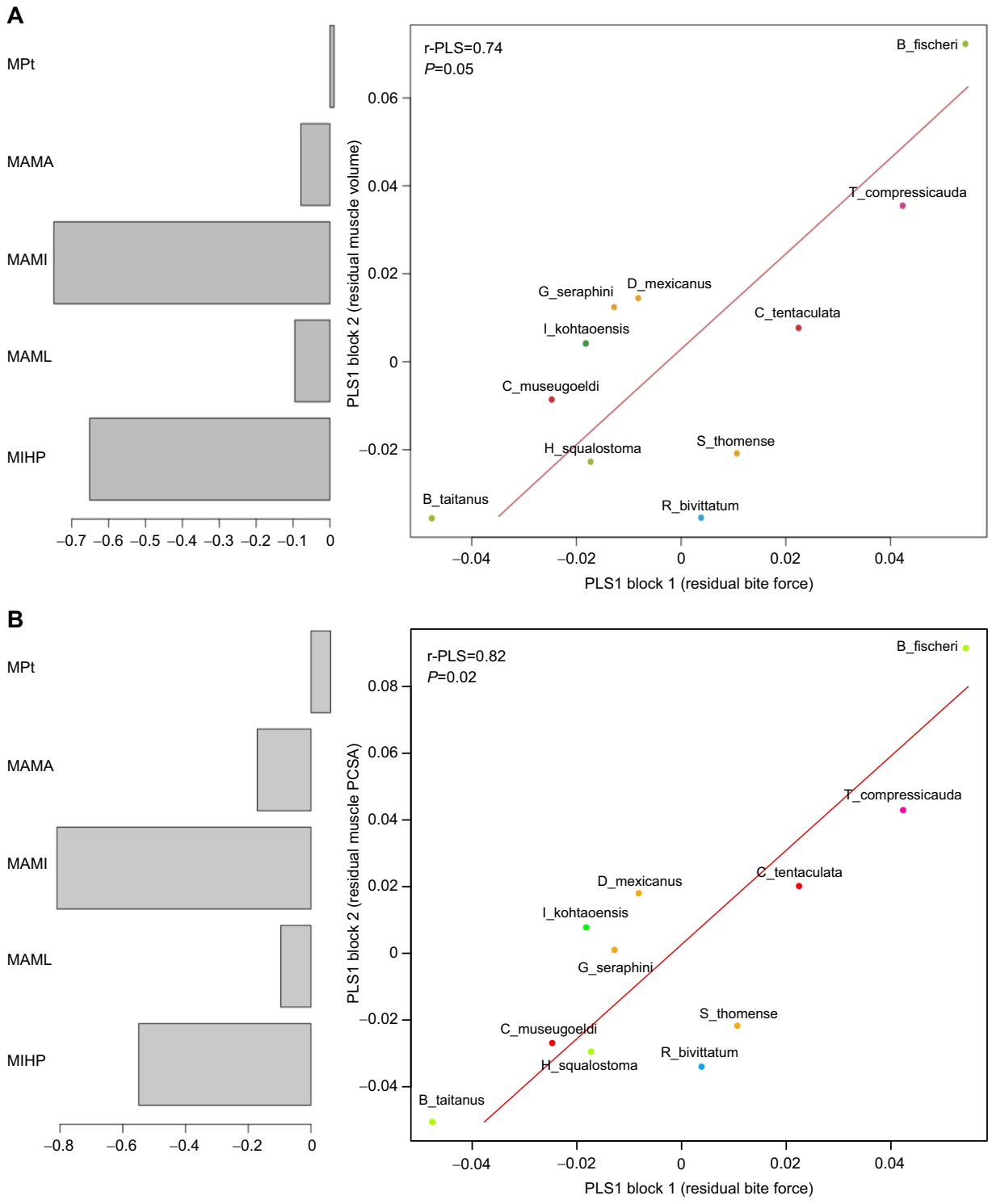

Fig. 5. Results of the phylogenetic 2B-PLS analysis of the residuals of muscle volume (*n*=44) and residual bite force (*n*=139), and muscle PCSA (*n*=44) and residual bite force (*n*=139). (A) Scatter plot of the first PLS axis describing the covariation between residuals of muscle volume and residual bite force. (B) Scatter plot of the first PLS axis describing the covariation between residuals of muscle PCSA and residual bite force. Circles represent species means (*n*=11) and are colored by clade. Loadings associated with the residual force covariation are represented by the histogram to the left of the scatterplot. MIHP, m. interhyoideus posterior; MAML, m. adductor mandibulae longus; MAMI, m. adductor mandibulae internus; MAMA, m. adductor mandibulae articularis; MPt, m. pterygoideus. For full species names, see Table 1.

curvature and length of the retroarticular process, along with the potential movement of the quadrate–squamosal complex (streptostyly), showed that these features have consequences for the biomechanics of jaw closure and can amplify bite force in caecilians (Summers and Wake, 2005). Moreover, as previously shown by Herrel et al. (2019) and hypothesized by O'Reilly (2000) and Summers and Wake (2005), bite force is also highly dependent on gape distance. Although some species appear to be able to

Journal of Experimental Biology (2022) 225, jeb243599. doi:10.1242/jeb.243599

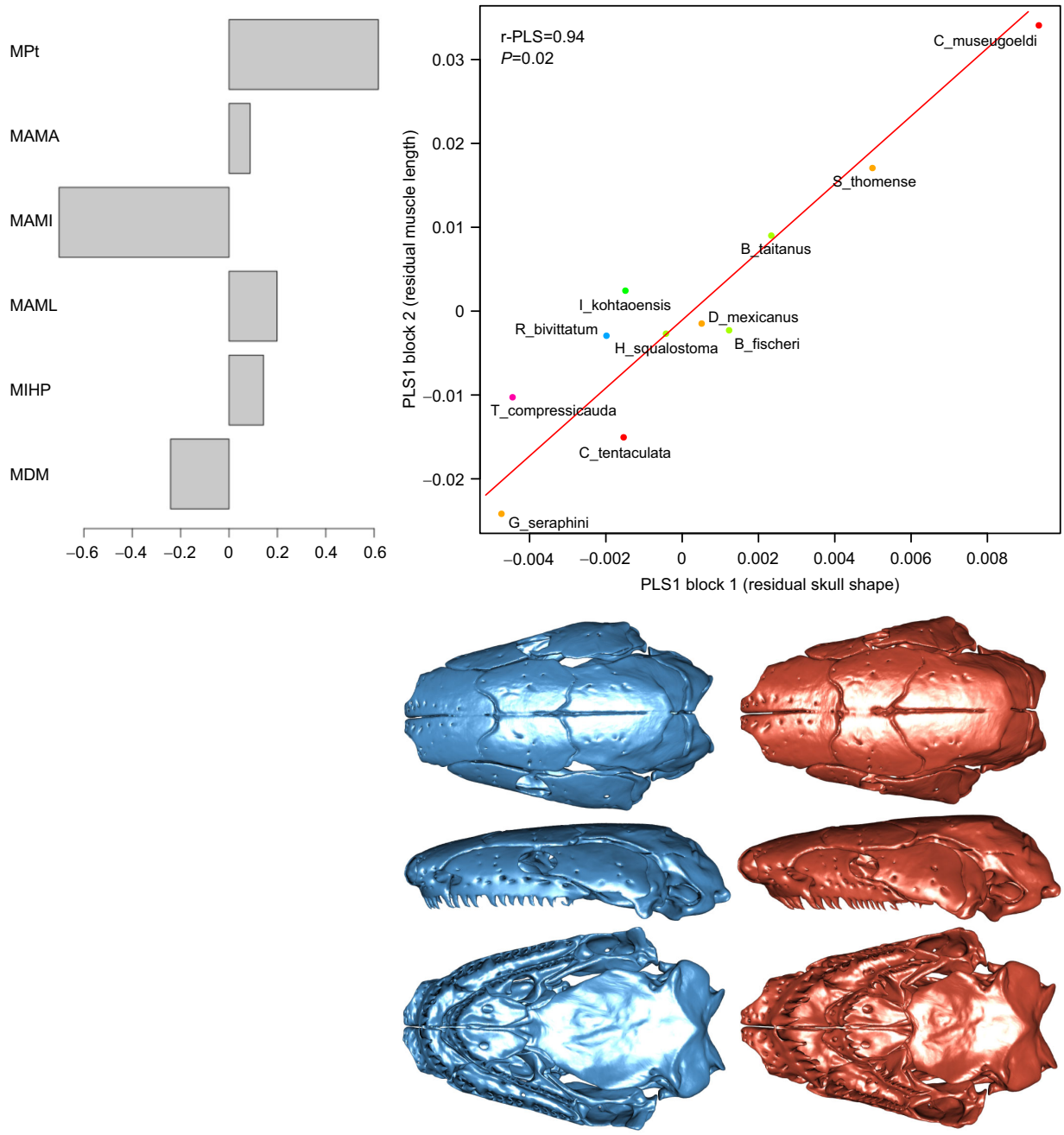

Fig. 6. Results of the phylogenetic 2B-PLS analysis of the residuals of muscle length (*n*=44) and residual cranial shape (*n*=81). Scatter plot of the first PLS axis describing the covariation between residuals of muscle length and residual cranial shape. Circles represent species means (*n*=11) and are colored by clade. Loadings associated with the residual shape covariation are represented by the histogram to the left of the scatterplot. MDM, m. depressor mandibulae; MIHP, m. interhyoideus posterior; MAML, m. adductor mandibulae longus, MAMI, m. adductor mandibulae internus; MAMA, m. adductor mandibulae articularis; MPt, m. pterygoideus. For full species names, see Table 1.

maintain bite force across different gape distances, a decrease in bite force was observed with increasing gape in others (Herrel et al., 2019). Species with a dorsoventrally curved retroarticular process have a better mechanical advantage for the MIHP at low gape (O'Reilly, 2000; Summers and Wake, 2005). In contrast, species with a retroarticular process in line with the pseudodentary are expected to perform poorly at low gape. Although the only aquatic species included in our bite force analysis, *Typhlonectes compressicauda*, did indeed show the lowest bite force for a given head width, no general relationship between *in vivo* bite force and mandible shape was found. Future studies on bite force at different gape distances are essential to fully understand the jaw-closing mechanisms in caecilians.

Relationship between shape and musculature

To date, no study has assessed the relationship between cranial musculature and skull shape in caecilians. However, this information is crucial to fully understand the evolution of the musculoskeletal system and the significance of morphological traits in driving variation in cranial function. As previously observed, the external adductors are architecturally constrained by size in the cranium. A complete coverage of the temporal region

Journal of Experimental Biology (2022) 225, jeb243599. doi:10.1242/jeb.243599

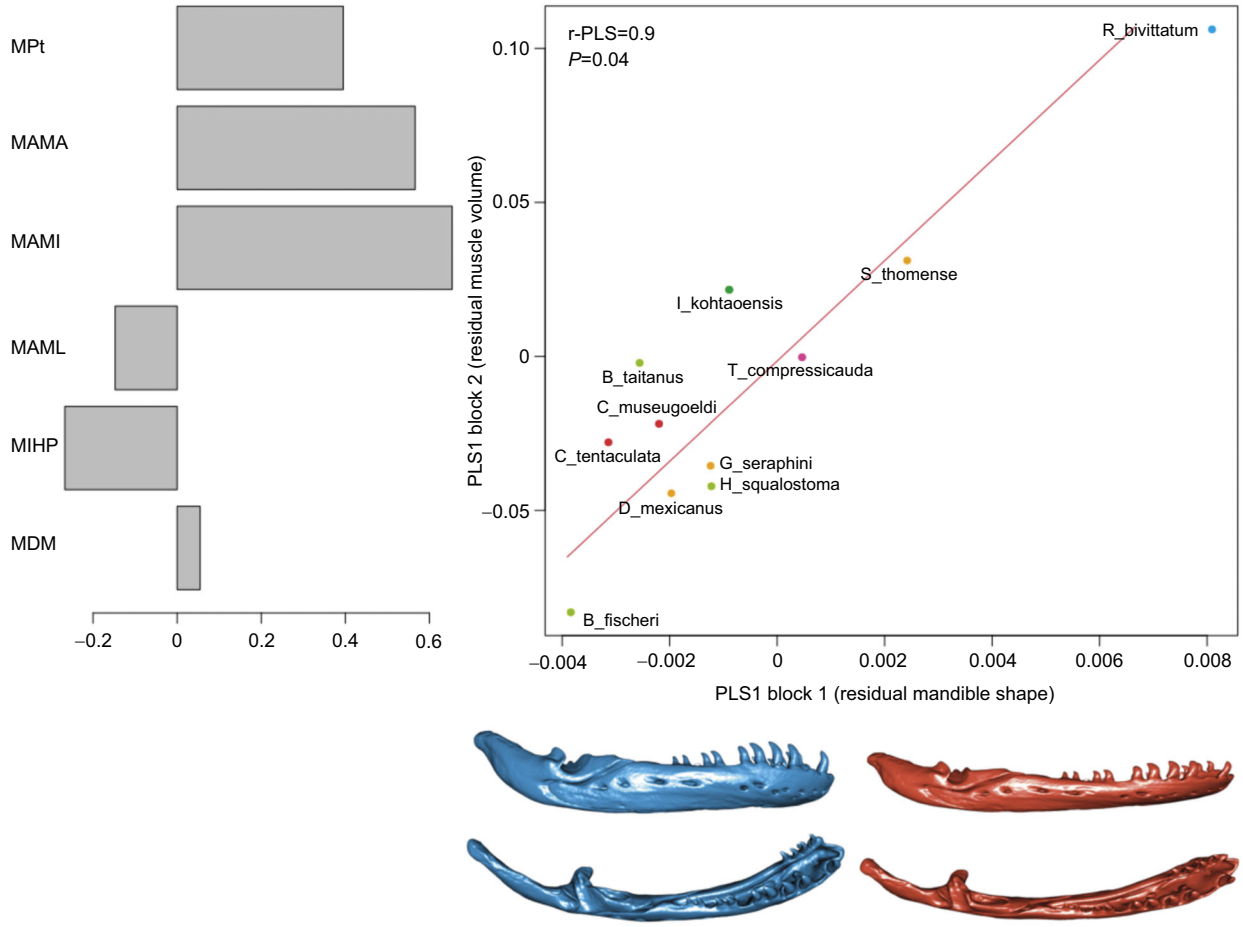

Fig. 7. Results of the phylogenetic 2B-PLS analysis of the residuals of muscle volume (*n*=44) and residual mandibular shape (*n*=139). Scatter plot of the first PLS axis describing the covariation between residuals of muscle volume and residual mandibular shape. Circles represent species means (*n*=11) and are colored by clade. Loadings associated with the residual shape covariation are represented by the histogram to the left of the scatterplot. MDM, m. depressor mandibulae; MIHP, m. interhyoideus posterior; MAML, m. adductor mandibulae longus; MAMI, m. adductor mandibulae internus; MAMA, m. adductor mandibulae articularis; MPt, m. pterygoideus. For full species names, see Table 1.

(stegokrotaphy) may limit the expansion of the muscles between the squamosal and the maxillopalatine (Bemis et al., 1983; Nussbaum, 1977, 1983; O'Reilly, 2000). As mentioned previously (Kleinteich et al., 2008b; Nussbaum, 1983; O'Reilly, 2000), the proportions of the different jaw-closing muscles are variable across species, suggesting that different feeding mechanisms may exist. We thus hypothesized that cranial shape would covary with the volume of the different head muscles in caecilians. However, only muscle length covaried with skull shape, suggesting that the organization of the jaw muscles is constrained mostly in length rather than in volume. Muscle length is important and will impact jaw-closing velocity and as such it would be of interest to better understand whether species differ in jaw-closing velocity (Herrel and Measey, 2012). The only study of feeding in these animals in their burrows (Herrel and Measey, 2012) suggested rapid jaw closure, possibly putting a premium on muscle fiber length, especially of the MAMI, which is ideally positioned to generate rapid jaw closure (Summers and Wake, 2005).

Because the large MIHP inserts on the retroarticular process (Bemis et al., 1983; Nussbaum, 1977, 1983), a covariation between mandibular shape and muscle PCSA was expected. However, only the volume of the muscles covaried with mandibular shape, suggesting that rather than the shape of the mandible being constrained by the forces exerted, it is the shape of the mandible that constrains the volume of the muscles that can insert upon it. Interestingly, species with a longer and more robust retroarticular process (e.g. *Boulengerula fischeri*) have a larger MIHP than species with a small retroarticular process (e.g. *Rhinatrema bivittatum*), the latter relying more on the jaw adductors for generating bite force. As the MIHP inserts on the retroarticular process, it makes sense that a longer retroarticular process provides a larger insertion area for the MIHP. Moreover, species with a longer retroarticular process appear to invest less in the traditional jaw adductors, which is reflected in a relatively shorter pseudoangular. The covariation observed does indeed suggest a continuum between species that invest in a large MIHP and that have a long retroarticular process versus those that invest in the 'traditional' jaw adductors and that have a rather short retroarticular process and a longer pseudoangular and deeper mandibular fossa.

The head musculature in caecilians is very different from that of other amphibians. Apart from their unique and transformed MIHP, caecilians also possess muscles that are not present in other amphibians, i.e. a true MPt and, in some, the m. levator quadrati (Kleinteich and Haas, 2007). Because caecilians also use rotational feeding to reduce prey (Measey and Herrel, 2006), these muscles could also play a role in stabilizing the jaw joint to avoid potential dislocation of the jaw during long-axis body rotation inside tunnels.

Clearly, a deeper understanding of the variation in the jaw muscles in caecilians is needed. Moreover, quantitative data on the architecture of the jaw muscles would permit the creation of accurate multibody dynamic models allowing the functional role of the different muscle groups to be tested.

Relationship between bite force and musculature

The streptostyly and the unique jaw-closing system in caecilians suggest that these animals can generate relatively high bite forces at low gape distances (Kleinteich et al., 2008b; Summers and Wake, 2005). Large bite forces are usually associated with the consumption of large or hard prey (e.g. Herrel et al., 2002, 2004; Edwards et al., 2013). However, only a few studies reported large prey in the diet of caecilians such as lizards and snakes, among others (Govindappa and Parwar, 2016; Moll and Smith, 1967; Presswell et al., 2002). Moreover, the use of rotational feeding would further suggest no requirement for very large bite forces. Indeed, the interlocking rows of sharp teeth probably maintain the jaws in a closed and locked position when feeding on soft large prey.

However, as suggested by previous studies (Herrel et al., 2019; Measey and Herrel, 2006), our results show that caecilians can generate considerable bite forces at relatively low gape angles for a given head width. Our study shows that higher bite forces are correlated with the overall size of the animal and the size of its head, a pattern also observed in other burrowing tetrapods (e.g. Le Guilloux et al., 2021; Vanhooydonck et al., 2011). Our results further show that bite force covaries with the volume and cross-sectional area of the MAMI and the MIHP. Whereas the important role of the MIHP was expected, that of the MAMI was less so (but see Kleinteich et al., 2008b). However, the MIHP is involved in multiple functions, whereas the adductors are exclusively involved in generating bite force. Indeed, the MIHP is also used in other functions such as buccal oscillation, ventilation and burrowing (Bemis et al., 1983; Nussbaum, 1983; Herrel et al., 2019). The strong covariation of bite force with the adductors suggests that the space available for this muscle may be one of the principal drivers of variation in bite force. Consequently, even small increases in the volume of the muscle may have a disproportionate impact on bite force. As shown by Herrel and Measey (2012), lunges and jaw closing are relatively fast. The longer and parallel-fibered muscles, such as the adductors, may shorten more rapidly and thus increase the velocity of the jaws. In contrast, bipennate muscles composed of shorter fibers such as the MIHP are known to produce more force to the detriment of velocity (Nussbaum, 1983; Summers and Wake, 2005). The combination of the two systems could allow caecilians to bite either forcefully or rapidly, providing them with a versatile jaw system (Summers and Wake, 2005).

Conclusions

Although bite force is correlated with external head measurements, our results suggest that the shape of the skull in caecilians is constrained more by other factors than by demands for bite force generation. However, the strong covariation between cranial and mandibular shapes and their covariation with respective muscle length and muscle volume suggests a continuum between species with long retroarticular processes that invest in large and forceful MIHP versus species with short retroarticular processes that invest in the traditional, but faster, long and parallel-fibered jaw adductors. Moreover, bite force mainly covaries with the volume and the PCSA of the MAMI, suggesting that the space available for this muscle might be driving bite force variation in caecilians. These results highlight the complexity of the jaw system and demonstrate that further studies including other parameters such as jaw velocity or gape distance are needed to fully understand feeding mechanics in caecilians.

Acknowledgements

We thank I. Josipovic and the people at Centre for X-Ray Tomography at Ghent University for their help with CT scanning. We thank the Natural History Museum (London), Museum of Zoology (University of Michigan), the Amphibian & Reptile Diversity Research Centre (University of Texas Arlington), the Royal Museum of Central Africa (Brussels), the Zoological Museum (Hamburg), A. Kupfer and the Staatliches Museum für Naturkunde Stuttgart and all the curators in these institutions for the loan of some key specimens. We also thank MorphoSource for making scans available. A.L. thanks A.-C. Fabre and M. Zelditch for their helpful discussions on the statistical analyses. A.L. also thanks M. H. Wake for the gift of *Dermophis* specimens.

Competing interests

The authors declare no competing or financial interests.

Author contributions

Conceptualization: A.L., D.A., A.H.; Methodology: A.L.; Formal analysis: A.L.; Investigation: A.L., A.H.; Resources: A.L., B.D., M.W., J.M., J.C.O., N.J.K., P.G., J.B., T.K., A.H.; Data curation: A.L., B.D.; Writing - original draft: A.L.; Writing - review & editing: A.L., B.D., M.W., J.M., J.C.O., N.J.K., P.G., J.B., T.K., D.A., A.H.; Visualization: A.L., D.A.; Supervision: D.A., A.H.; Project administration: D.A., A.H.; Funding acquisition: A.L., J.M.

Funding

This study was supported by the Research Foundation, Flanders (Fonds Wetenschappelijk Onderzoek, grant 11D5819N), a TOURNESOL travel grant, the Royal Belgian Zoological Society and a European Union Marie Curie Fellowship (HPMF-CT-2001-01407), and field work and visiting fellowship of the Fonds Wetenschappelijk Onderzoek, Flanders, Belgium (FWO-VI) to J.M. The special research fund of Ghent University (Bijzonder Onderzoeksfonds UGent, BOF-UGent) is acknowledged for financial support of the UGCT Centre of Expertise (BOF.EXP.2017.0007).

References

Adams, D. C. (2014). A generalized K statistic for estimating phylogenetic signal from shape and other high-dimensional multivariate data. *Syst. Biol.* **63**, 685-697. doi:10.1093/sysbio/syu030

Bardua, C., Felice, R. N., Watanabe, A., Fabre, A. and Goswami, A. (2019a). A practical guide to sliding and surface semilandmarks in morphometric analyses. *Integr. Org. Biol.* **1**, 1-34. doi:10.1093/iob/obz016

Bardua, C., Wilkinson, M., Gower, D. J., Sherratt, E. and Goswami, A. (2019b). Morphological evolution and modularity of the caecilian skull. *BMC Evol. Biol.* **19**, 1-24. doi:10.1186/s12862-018-1342-7

Bemis, W. E., Schwenk, K. and Wake, M. H. (1983). Morphology and function of the feeding apparatus in *Dermophis mexicanus* (Amphibia: Gymnophiona). *Zool. J. Linn. Soc.* **77**, 75-96. doi:10.1111/j.1096-3642.1983.tb01722.x

Blomberg, S. P., Garland, T. and Ives, A. R. (2003). Testing for phylogenetic signal in comparative data: behavioral traits are more labile. *Evolution* **57**, 717-745. doi:10.1111/j.0014-3820.2003.tb00285.x

Bookstein, F. (1991). *Morphometric Tools for Landmark Data: Geometry and Biology*. Cambridge: Cambridge University Press.

Botton-Divet, L., Cornette, R., Fabre, A., Herrel, A. and Houssaye, A. (2016). Morphological analysis of long bones in semi-aquatic mustelids and their terrestrial relatives. *Integr. Comp. Biol.* **56**, 1298-1309. doi:10.1093/icb/icw124

Buser, T. J., Sidlauskas, B. L. and Summers, A. P. (2018). 2D or not 2D? Testing the utility of 2D vs. 3D landmark data in geometric morphometrics of the sculpin subfamily Oligocottinae (Pisces; Cottoidea). *Anat. Rec.* **301**, 806-818. doi:10.1002/ar.23752

Carrier, D. R. and Wake, M. H. (1995). Mechanism of lung ventilation in the caecilian *Dermophis mexicanus*. *J. Morphol.* **226**, 289-295. doi:10.1002/jmor.1052260305

Delêtre, M. and Measey, G. J. (2004). Sexual selection vs ecological causation in a sexually dimorphic caecilian, *Schistometopum thomense* (Amphibia Gymnophiona Caeciliidae). *Ethol. Ecol. Evol.* **16**, 243-253. doi:10.1080/08927014.2004.9522635

Descamps, E., Sochacka, A., de Kegel, B., Van Loo, D., Hoorebeke, L. and Adriaens, D. (2014). Soft tissue discrimination with contrast agents using micro-ct scanning. *Belgian J. Zool.* **144**, 20-40. doi:10.26496/bjz.2014.63

Ducey, P. K., Formanowicz, D. R. J., Boyet, L., Mailloux, J. and Nussbaum, R. A. (1993). Experimental examination of burrowing behavior in caecilians (Amphibia: Gymnophiona): effects of soil compaction on burrowing ability of four species. *Herpetologica* **49**, 450-457.

Edwards, S., Tolley, K. A., Vanhooydonck, B., Measey, G. J. and Herrel, A. (2013). Is dietary niche breadth linked to morphology and performance in Sandveld lizards nucras (Sauria: Lacertidae)? *Biol. J. Linn. Soc.* **110**, 674-688. doi:10.1111/bij.12148

Fabre, A. C., Cornette, R., Goswami, A. and Peigné, S. (2015). Do constraints associated with the locomotor habitat drive the evolution of forelimb shape? A case study in musteloid carnivorans. *J. Anat.* **226**, 596-610. doi:10.1111/joa.12315

Fabre, A. C., Perry, J. M. G., Hartstone-Rose, A., Lowie, A., Boens, A. and Dumont, M. (2018). Do muscles constrain skull shape evolution in strepsirrhines? *Anat. Rec.* **301**, 291-310. doi:10.1002/ar.23712

Felsenstein, J. (1985). Phylogenies and the comparative method. *Am. Nat.* **125**, 1-15. doi:10.1086/284325

Gaborieau, O. and Measey, G. J. (2004). Termitivore or detritivore? A quantitative investigation into the diet of the East African caecilian *Boulengerula taitanus* (Amphibia: Gymnophiona: Caeciliidae). *Anim. Biol.* **54**, 45-56. doi:10.1163/157075604323010042

Gans, C. (1974). *Biomechanics. An Approach to Vertebrate Biology*. Philadelphia: J.B. Lippincott Company.

Gignac, P. M., Kley, N. J., Clarke, J. A., Colbert, M. W., Morhardt, A. C., Cerio, D., Cost, I. N., Cox, P. G., Daza, J. D., Early, C. M. et al. (2016). Diffusible iodine-based contrast-enhanced computed tomography (diceCT): an emerging tool for rapid, high-resolution, 3-D imaging of metazoan soft tissues. *J. Anat.* **228**, 889-909. doi:10.1111/joa.12449

Govindappa, V. and Parwar, S. (2016). An unusual diet of *Ichthyophis* caecilians (Amphibia : Gymnophiona). *Curr. Sci.* **111**, 793-795. doi:10.1016/j.corsci.2016.05.009

Gunz, P., Mitteroecker, P. and Bookstein, F. L. (2005). Semilandmarks in three dimensions. In *Modern Morphometrics in Physical Anthropology* (ed. D. E. Slice), pp. 73-98. Boston, MA: Springer US.

Haas, A. (2001). Mandibular arch musculature of anuran tadpoles, with comments on homologies of amphibian jaw muscles. *J. Morphol.* **247**, 1-33. doi:10.1002/1097-4687(200101)247:1<1::AID-JMOR1000>3.0.CO;2-3

Herrel, A. and Measey, G. J. (2010). The kinematics of locomotion in caecilians: effects of substrate and body shape. *J. Exp. Zool. Part A Ecol. Genet. Physiol.* **313A**, 301-309. doi:10.1002/jez.599

Herrel, A. and Measey, G. J. (2012). Feeding underground: kinematics of feeding in caecilians. *J. Exp. Zool. Part A Ecol. Genet. Physiol.* **317**, 533-539. doi:10.1002/jez.1745

Herrel, A., Spithoven, L., Van Damme, R. and De Vree, F. (1999). Sexual dimorphism of head size in Gallotia galloti: testing the niche divergence hypothesis by functional analyses. *Funct. Ecol.* **13**, 289-297. doi:10.1046/j.1365-2435.1999.00305.x

Herrel, A., Van Damme, R., Vanhooydonck, B. and De Vree, F. (2001). The implications of bite performance for diet in two species of lacertid lizards. *Can. J. Zool.* **79**, 662-670. doi:10.1139/z01-031

Herrel, A., O'Reilly, J. C. and Richmond, A. M. (2002). Evolution of bite performance in turtles. *J. Evol. Biol.* **15**, 1083-1094. doi:10.1046/j.1420-9101.2002.00459.x

Herrel, A., Vanhooydonck, B. and Van Damme, R. (2004). Omnivory in lacertid lizards: adaptive evolution or constraint? *J. Evol. Biol.* **17**, 974-984. doi:10.1111/j.1420-9101.2004.00758.x

Herrel, A., Reilly, J. C. O., Fabre, A., Bardua, C., Lowie, A., Boistel, R. and Gorb, S. N. (2019). Feeding in amphibians: evolutionary transformations and phenotypic diversity as drivers of feeding system diversity. In *Feeding in Vertebrates* (ed. V. Bels and I. Q. Whishaw), pp. 431-467. Cham, Switzerland: Springer Nature.

Jetz, W. and Pyron, R. A. (2018). The interplay of past diversification and evolutionary isolation with present imperilment across the amphibian tree of life. *Nat. Ecol. Evol.* **2**, 850-858. doi:10.1038/s41559-018-0515-5

Kamei, R. G., San Mauro, D., Gower, D. J., Van Bocxlaer, I., Sherratt, E., Thomas, A., Babu, S., Bossuyt, F., Wilkinson, M. and Biju, S. D. (2012). Discovery of a new family of amphibians from northeast India with ancient links to Africa. *Proc. R. Soc. B Biol. Sci.* **279**, 2396-2401. doi:10.1098/rspb.2012.0150

Kleinteich, T. and Haas, A. (2007). Cranial musculature in the larva of the caecilian, *Ichthyophis kohtaoensis* (Lissamphibia: Gymnophiona). *J. Morphol.* **268**, 74-88. doi:10.1002/jmor.10503

Kleinteich, T., Beckmann, F., Herzen, J., Summers, A. P. and Haas, A. (2008a). Applying x-ray tomography in the field of vertebrate biology: form, function, and evolution of the skull of caecilians (Lissamphibia: Gymnophiona). *Proc. SPIE* **7078**, 70780D. doi:10.1117/12.795063

Kleinteich, T., Haas, A. and Summers, A. P. (2008b). Caecilian jaw-closing mechanics: integrating two muscle systems. *J. R. Soc. Interface* **5**, 1491-1504. doi:10.1098/rsif.2008.0155

Kleinteich, T., Maddin, H. C., Herzen, J., Beckmann, F. and Summers, A. P. (2012). Is solid always best? Cranial performance in solid and fenestrated caecilian skulls. *J. Exp. Biol.* **215**, 833-844. doi:10.1242/jeb.065979

Kouete, M. T. and Blackburn, D. C. (2020). Dietary partitioning in two co-occurring caecilian species (*Geotrypetes seraphini* and *Herpele squalostoma*) in Central Africa. *Integr. Org. Biol.* **2**, obz035. doi:10.1093/iob/obz035

Kupfer, A. (2009). Sexual size dimorphism in caecilian amphibians: analysis, review and directions for future research. *Zoology* **112**, 362-369. doi:10.1016/j.zool.2008.12.001

Kupfer, A., Nabhitabhata, J. and Himstedt, W. (2005). From water into soil: trophic ecology of a caecilian amphibian (Genus *Ichthyophis*). *Acta Oecol.* **28**, 95-105. doi:10.1016/j.actao.2005.03.002

Le Guilloux, M., Miralles, A., Measey, J., Vanhooydonck, B., O'Reilly, J. C., Lowie, A. and Herrel, A. (2021). Trade-offs between burrowing and biting force in fossorial scincid lizards? *Biol. J. Linn. Soc.* **130**, 310-319. doi:10.1093/biolinnean/blaa031

Lowie, A., De Kegel, B., Wilkinson, M., Measey, J., O'Reilly, J. C., Kley, N. J., Gaucher, P., Brecko, J., Kleinteich, T., Van Hoorebeke, L. et al. (2021). Under pressure: the relationship between cranial shape and burrowing force in caecilians (Gymnophiona). *J. Exp. Biol.* **224**, jeb242964. doi:10.1242/jeb.242964

Maerker, M., Reinhard, S., Pogoda, P. and Kupfer, A. (2016). Sexual size dimorphism in the viviparous caecilian amphibian *Geotrypetes seraphini* seraphini (Gymnophiona: Dermophiidae) including an updated overview of sexual dimorphism in caecilian amphibians. *Amphib. Reptil.* **37**, 291-299. doi:10.1163/15685381-00003057

Masschaele, B., Dierick, M., Van Loo, D., Boone, M. N., Brabant, L., Pauwels, E., Cnudde, V. and Van Hoorebeke, L. (2013). HECTOR: A 240kV micro-CT setup optimized for research. *J. Phys. Conf. Ser.* **463**, 012012. doi:10.1088/1742-6596/463/1/012012

Measey, G. J. and Herrel, A. (2006). Rotational feeding in caecilians: putting a spin on the evolution of cranial design. *Biol. Lett.* **2**, 485-487. doi:10.1098/rsbl.2006.0516

Measey, G. J., Gower, D. J., Oommen, O. V. and Wilkinson, M. (2004). A subterranean generalist predator: diet of the soil-dwelling caecilian *Gegeneophis ramaswamii* (Amphibia; Gymnophiona; Caeciliidae) in southern India. *Comptes Rendus Biol.* **327**, 65-76. doi:10.1016/j.crvi.2003.11.001

Mendez, J. and Keys, A. (1960). Density and composition of mammalian muscle. *Metabolism* **9**, 184-188.

Moll, E. O. and Smith, H. M. (1967). Lizards in the diet of an American caecilian. *Nat. Hist. Misc. Chicago Acad. Sci.* **187**, 1-2.

Nussbaum, R. A. (1977). Rhinatrematidae: a new family of caecilians (Amphibia: Gymnophiona). *Occas. Pap. Museum Zool.* **682**, 1-30.

Nussbaum, R. A. (1983). The evolution of a unique dual jaw–closing mechanism in caecilians (Amphibia: Gymnophiona) and its bearing on caecilian ancestry. *J. Zool., Lond.* **199**, 545-554. doi:10.1111/j.1469-7998.1983.tb05105.x

O'Reilly, J. C. (2000). Feeding in caecilians. In *Feeding: Form, Function, and Evolution in Tetrapod Vertebrates* (ed. K. Schwenk), pp. 149-166. Academic Press.

Pough, F. H., Andrews, R. M., Cadle, J. E., Crump, M. L., Savitzky, A. H. and Wells, K. D. (1998). *Herpetology*. New Jersey: Prentice-Hall.

Presswell, B., Gower, D. J., Oomen, O. V., Measey, G. J. and Wilkinson, M. (2002). Scolecophidian snakes in the diets of South Asian caecilian amphibians. *Herpetol. J.* **12**, 123-126.

Sherratt, E., Gower, D. J., Klingenberg, C. P. and Wilkinson, M. (2014). Evolution of cranial shape in caecilians (Amphibia: Gymnophiona). *Evol. Biol.* **41**, 528-545. doi:10.1007/s11692-014-9287-2

Summers, A. P. and O'Reilly, J. C. (1997). A comparative study of locomotion in the caecilians *Dermophis mexicanus* and *Typhlonectes natans* (Amphibia: Gymnophiona). *Zool. J. Linn. Soc.* **121**, 65-76. doi:10.1111/j.1096-3642.1997.tb00147.x

Summers, A. P. and Wake, M. H. (2005). The retroarticular process, streptostyly and the caecilian jaw closing system. *Zoology* **108**, 307-315. doi:10.1016/j.zool.2005.09.007

Taylor, E. H. (1968). *The Caecilians of the World. A Taxonomic Review*. Lawrence: University of Kansas Press.

Theska, T., Mark, W., Gower, D. J. and Mueller, H. (2018). Musculoskeletal development of the Central African caecilian *Idiocranium russeli* (Amphibia: Gymnophiona: Indotyphlidae) and its bearing on the re-evolution of larvae in caecilian amphibians. *Zoomorphology* **138**, 137-158. doi:10.1007/s00435-018-0420-0

Vanhooydonck, B., Boistel, R., Fernandez, V. and Herrel, A. (2011). Push and bite: trade-offs between burrowing and biting in a burrowing skink (*Acontias percivali*). *Biol. J. Linn. Soc.* **102**, 91-99. doi:10.1111/j.1095-8312.2010.01563.x

Verdade, V. K., Schiesari, L. C. and Bertoluci, J. A. (2000). Diet of juvenile aquatic caecilians, *Typhlonectes compressicauda*. *J. Herpetol.* **34**, 291-293. doi:10.2307/1565428

Wake, M. H. (1980). Reproduction, growth, and population structure of the Central American caecilian *Dermophis mexicanus*. *Herpetologica* **36**, 244-256.

Wake, M. H. (1993). The skull as a locomotor organ. In *The Skull: Functional and Evolutionary Mechanisms* (ed. J. Hanken and B. K. Hall), pp. 197-240. Chicago, IL, USA: University of Chicago Press.

Wake, M. H. (2003). The osteology of caecilians. In *Amphibian Biology: Osteology*, Vol. 5 (ed. H. Heatwole and M. Davies), pp. 1809-1876. Chipping Norton: Surrey Beatty and Sons.

Wake, M. H. and Hanken, J. (1982). Development of the skull of *Dermophis mexicanus* (Amphibia: Gymnophiona), with comments on skull kinesis and amphibian relationships. *J. Morphol.* **173**, 203-223. doi:10.1002/jmor.1051730208

Wilkinson, M. (2012). Caecilians. *Curr. Biol.* **22**, 668-669. doi:10.1016/j.cub.2012.06.019

Wilkinson, M. and Nussbaum, R. A. (1997). Comparative morphology and evolution of the lungless caecilian *Atretochoana eiselti* (Taylor) (Amphibia: Gymnophiona: Typhlonectidae). *Biol. J. Linn. Soc.* **62**, 39-109.

Wilkinson, M., Mauro, D. S., Sherratt, E. and Gower, D. J. (2011). A nine-family classification of caecilians (Amphibia: Gymnophiona). *Zootaxa* **64**, 41-64. doi:10.11646/zootaxa.2874.1.3

Table S1. Details of the specimens/scans used in the study.

Family	Species	ID	Origin	Voxel size (µm)
Caeciliidae	*Caecilia museugoeldi**	V2101	NHM	17.65
	*Caecilia tentaculata**	3955	NHM	22.93
	Caecilia tentaculata	ku:kuh:175441	MS	41.8
Dermophiidae	*Dermophis mexicanus*	cas:herp:144523	MS	50.79
	*Dermophis mexicanus**	A-52188	UTACV	23.05
	*Dermophis mexicanus**	AL2101201	AL	25.63
	*Dermophis mexicanus**	AL2101202	AL	22.55
	*Geotrypetes seraphini**	2	AH	17.3
	*Geotrypetes seraphini**	6	AH	15.17
	*Geotrypetes seraphini**	AL1	AH	16
	*Geotrypetes seraphini**	AL21	AH	13.77
	*Geotrypetes seraphini**	AL5	AH	15.17
	Schistometopum gregorii	cas:herp:245198	MS	27.28
	*Schistometopum thomense**	6	AH	14.17
	*Schistometopum thomense**	7	AH	13.69
	*Schistometopum thomense**	#8	AH	16
	*Schistometopum thomense**	AL11	AH	13.99
Herpelidae	*Boulengerula boulengeri*	fmnh:amphibians and reptiles:251369	MS	23.74
	*Boulengerula fischeri**	3	AH	14.48
	*Boulengerula fischeri**	4	AH	8.67
	*Boulengerula fischeri**	5	AH	9.8
	*Boulengerula fischeri**	7	AH	9.06
	*Boulengerula fischeri**	AH1	AH	9.74
	*Boulengerula taitanus**	AH2	AH	16.07
	*Boulengerula taitanus**	AL010401	AH	11.7
	*Boulengerula taitanus**	AL010402	AH	9.94
	*Boulengerula taitanus**	JM01452	AH	12.23
	*Boulengerula taitanus**	JM01584	AH	12.23
	*Herpele squalostoma**	AL10	AH	14.34
	*Herpele squalostoma**	AL2	AH	16
	*Herpele squalostoma**	AL30	AH	11.75
	*Herpele squalostoma**	AL31	AH	13.53
	*Herpele squalostoma**	AL32	AH	15.4
Ichthyophiidae	*Ichthyophis bombayensis*	uf:herp:76734	MS	15.72
	Ichthyophis kohtaoensis	ncsm:herp:79205	MS	18.01
	Ichthyophis kohtaoensis	ZMH A08981	ZMH	6.83
	*Ichthyophis kohtaoensis**	218831	UMMZ	14.29
	*Ichthyophis kohtaoensis**	218832	UMMZ	13.64
	Uraeotyphlus oxyurus	uf:herp:62870	MS	15.41
Indotyphlidae	*Gegeneophis ramaswamii*	151	NHM	6.52
	Gegeneophis ramaswamii	616	NHM	6.57

	Gegeneophis ramaswamii	654	NHM	6.57
	Gegeneophis ramaswamii	1275	NHM	8.5
	Grandisonia alternans	109185	RMCA	12.58
	Grandisonia alternans	109186	RMCA	11.79
	Grandisonia alternans	109187	RMCA	10.59
	Grandisonia alternans	cas:herp:157086	MS	44.98
	Hypogeophis rostratus	73_38_B_101	RMCA	8.61
	Hypogeophis rostratus	73_38_B_110	RMCA	9.73
	Hypogeophis rostratus	73_38_B_111	RMCA	10.33
	Hypogeophis rostratus	73_48_B_1	RMCA	9.6
	Sylvacaecilia grandisonae	ummz:herps:227904	MS	13.5
Rhinatrematidae	*Epicrionops bicolor*	lsumz:herps:27295	MS	13.14
	Rhinatrema bivittatum	byu:main:48675	MS	12.81
	*Rhinatrema bivittatum**	A53	AH	16
	*Rhinatrema bivittatum**	AL8	AH	16.69
	*Rhinatrema bivittatum**	B75	AH	11.28
	*Rhinatrema bivittatum**	B80	AH	28.34
Scolecomorphidae	*Scolecomorphus kirkii*	101889	RMCA	5.35
	Scolecomorphus uluguruensis	11102	RMCA	7.25
	Scolecomorphus uluguruensis	101890	RMCA	6.2
	Scolecomorphus uluguruensis	101891	RMCA	7.44
	Scolecomorphus uluguruensis	101892	RMCA	8.07
	Scolecomorphus uluguruensis	101894	RMCA	6.97
	Scolecomorphus uluguruensis	101896	RMCA	6.78
Siphonopidae	*Microcaecilia unicolor*	MU1	NHM	7.23
	*Microcaecilia unicolor**	prey	AH	9.24
	Mimosiphonops vermiculatus	ku:kuh:93271	MS	16.02
	Siphonops annulatus	cas:herp:74304	MS	22.17
	Siphonops annulatus	1924_9_20_9_Redo	NHM	9.82
	Siphonops annulatus	ZMH A00235	ZMH	9.2
Typhlonectidae	*Atretochoana eiselti*	30919	AH	19.98
	Atretochoana eiselti	uf:herp:185560	MS	29
	Potomotyphlus kaupii	PotomoH2_01	NHM	9.71
	Potomotyphlus kaupii	PotomoH2_01	NHM	9.71
	Typhlonectes compressicauda	11307	NHM	8.4
	Typhlonectes compressicauda	cas:herp:125421	MS	36.87
	*Typhlonectes compressicauda**	AL20	AH	17.65
	*Typhlonectes compressicauda**	AL6	AH	19.41
	*Typhlonectes compressicauda**	AL7	AH	20.12
	Typhlonectes natans	ZMH A08984	ZMH	3.89

*Specimens scanned using the HECTOR micro computed tomography (µCT) scanner
Abbreviations are as follows:

Personal collection of Anthony Herrel (AH)
Personal collection of Aurélien Lowie (AL)
Morphosource.org (MS)
Natural History Museum, London (NHM)
Royal Museum of Central Africa (RMCA)
University of Michigan, Museum of Zoology (UMMZ)
University of Texas Arlington, Amphibian & Reptile Diversity Research Center (UTACV)
Zoological Museum, Hamburg (ZMH)

Table S2. Details of the stained specimens used in the study.

Family	Species	ID	Origin	Staining	Voxel size (µm)
Caeciliidae	*Caecilia museugoeldi*	V2101	NHM	I_2KI	16.61
	Caecilia tentaculata	3955	NHM	I_2KI	14.01
Dermophiidae	*Dermophis mexicanus*	A-52188	UTACV	PMA	9.58
	Geotrypetes seraphini	6	AH	PMA	4
	Schistometopum thomense	#8	AH	PMA	7.04
Herpelidae	*Boulengerula fischeri*	5	AH	PMA	5.49
	Boulengerula taitanus	JM01452	AH	PMA	7.04
	Herpele squalostoma	AL31	AH	PMA	10.49
Ichthyophiidae	*Ichthyophis kohtaoensis*	218831	UMMZ	I_2KI	6.41
Rhinatrematidae	*Rhinatrema bivittatum*	AL8	AH	PMA	9.59
Typhlonectidae	*Typhlonectes natans*	SMNS16297	SMNS	I_2KI	10

Abbreviations are as follows:
Personal collection of Anthony Herrel (AH)
Natural History Museum, London (NHM)
Staatliches Museum für Naturkunde Stuttgart (SMNS)
University of Michigan, Museum of Zoology (UMMZ)
University of Texas Arlington, Amphibian & Reptile Diversity Research Center (UTACV)

Table S3. Length, volume and PCSA of the species used in this study.

Species	L_MDM (mm)	L_MIHP (mm)	L_MAML (mm)	L_MAMI (mm)	L_MAMA (mm)	L_MPt (mm)
B_fischeri	1.179 ± 0.119	2.428 ± 0.277	0.736 ± 0.168	0.747 ± 0	0.48 ± 0	0.627 ± 0.18
B_taitanus	1.405 ± 0.318	2.306 ± 0.384	0.962 ± 0.082	0.669 ± 0.136	0.526 ± 0	0.886 ± 0.262
C_museugoeldi	2.243	4.158	2.03	0.895	1.178	2.233
C_tentaculata	4.816	6.656	3.507	2.464	1.714	3.12
D_mexicanus	4.027 ± 0.49	6.59 ± 0.732	3.178 ± 0.31	2.09 ± 0.264	1.585 ± 0.496	2.295 ± 0.976
G_seraphini	1.661 ± 0.47	2.836 ± 1.248	1.188 ± 0.419	1.179 ± 0.49	0.823 ± 0	0.528 ± 0.154
H_squalostoma	1.96 ± 0.291	2.595 ± 0.527	1.128 ± 0.134	0.903 ± 0.274	0.759 ± 0	0.914 ± 0.203
I_kohtaoensis	3.158 ± 0.18	4.737 ± 0.57	1.812 ± 0.1	1.477 ± 0.085	0.931 ± 0.113	1.8 ± 0.253
R_bivittatum	1.793 ± 0.524	2.342 ± 0.662	0.83 ± 0.222	1.075 ± 0.08	1.259 ± 0.164	1.033 ± 0.43
S_thomense	1.975 ± 0.271	3.629 ± 0.42	1.457 ± 0.354	0.839 ± 0.327	1.302 ± 0.661	1.069 ± 0.494
*T_compressicauda**	4.121 ± 1.05	4.079 ± 1.517	2.158 ± 0.426	1.862 ± 0.665	1.724 ± 0	1.656 ± 0.73

Species	V_MDM (mm^3)	V_MIHP (mm^3)	V_MAML (mm^3)	V_MAMI (mm^3)	V_MAMA (mm^3)	V_MPt (mm^3)
B_fischeri	0.188 ± 0.118	0.944 ± 0.356	0.101 ± 0.033	0.004 ± 0.001	0.003 ± 0.001	0.017 ± 0.012
B_taitanus	0.979 ± 0.252	5.964 ± 2.635	0.226 ± 0.11	0.101 ± 0.035	0.018 ± 0	0.056 ± 0.058
C_museugoeldi	3.859	45.129	2.236	0.366	0.167	1.311
C_tentaculata	19.624	200.886	8.041	2.237	1.121	5.055
D_mexicanus	18.593 ± 8.514	113.996 ± 65.291	7.749 ± 3.126	2.171 ± 0.986	0.654 ± 0.463	2.63 ± 1.32
G_seraphini	1.393 ± 0.535	5.615 ± 2.108	0.576 ± 0.162	0.141 ± 0.067	0.064 ± 0	0.047 ± 0.033
H_squalostoma	2.239 ± 0.925	24.311 ± 39.343	0.399 ± 0.133	0.145 ± 0.034	0.029 ± 0	0.142 ± 0.055
I_kohtaoensis	1.881 ± 0.189	7.791 ± 2.027	0.893 ± 0.412	0.42 ± 0.218	0.311 ± 0.108	0.935 ± 0.247
R_bivittatum	1.677 ± 0.707	1.985 ± 0.822	0.218 ± 0.07	1.875 ± 0.871	0.441 ± 0.16	0.858 ± 0.406
S_thomense	1.628 ± 0.981	6.67 ± 4.377	0.514 ± 0.4	0.225 ± 0.216	0.107 ± 0	0.163 ± 0.091
*T_compressicauda**	2.91 ± 1.117	14.601 ± 8.491	1.804 ± 1.126	0.569 ± 0.62	0.368 ± 0	1.744 ± 1.586

Species	PCSA_MDM (mm²)	PCSA_MIHP (mm²)	PCSA_MAML (mm²)	PCSA_MAMI (mm²)	PCSA_MAMA (mm²)	PCSA_MPt (mm²)
B_fischeri	0.154 ± 0.082	0.405 ± 0.188	0.141 ± 0.044	0.006 ± 0	0.007 ± 0	0.03 ± 0.023
B_taitanus	0.695 ± 0.061	2.699 ± 1.523	0.237 ± 0.114	0.152 ± 0.051	0.035 ± 0	0.055 ± 0.044
C_museugoeldi	1.721	10.853	1.101	0.41	0.142	0.587
C_tentaculata	4.074	30.18	2.293	0.908	0.654	1.62
D_mexicanus	4.542 ± 1.695	17.437 ± 9.865	2.393 ± 0.715	1.017 ± 0.355	0.454 ± 0.412	1.216 ± 0.55
G_seraphini	0.842 ± 0.208	2.349 ± 1.327	0.539 ± 0.235	0.139 ± 0.06	0.078 ± 0	0.093 ± 0.062
H_squalostoma	1.131 ± 0.378	9.832 ± 16.462	0.351 ± 0.105	0.171 ± 0.062	0.038 ± 0	0.16 ± 0.074
I_kohtaoensis	0.596 ± 0.056	1.653 ± 0.443	0.49 ± 0.213	0.279 ± 0.134	0.344 ± 0.151	0.522 ± 0.125
R_bivittatum	0.975 ± 0.381	0.92 ± 0.48	0.288 ± 0.162	1.736 ± 0.784	0.354 ± 0.145	0.873 ± 0.402
S_thomense	0.795 ± 0.384	1.799 ± 1.145	0.331 ± 0.183	0.242 ± 0.185	0.128 ± 0	0.151 ± 0.069
*T_compressicauda**	0.693 ± 0.148	3.421 ± 0.743	0.814 ± 0.397	0.258 ± 0.205	0.213 ± 0	0.922 ± 0.471

Data are means±s.d. MDM: *m. depressor mandibulae*, MIHP: *m. interhyoideus posterior*, MAML: *m. adductor mandibulae longus,* MAMI: *m. adductor mandibulae internus*, MAMA: *m. adductor mandibulae articularis*, MPt: *m. pterygoideus*. For the number of individuals used, see Table 1.

* Due to the scarcity of *Typhlonectes compressicauda* in the collections but the availability of *Typhlonectes natans*, the mean for *T. compressicauda* includes one specimen of *T. natans*. As the species are morphologically and phylogenetically close, we assumed that the data would not be biased by this addition.